

Supplementary Material for
**What Mn K_{β} Spectroscopy Reveals Concerning the Oxidation States of
the Mn Cluster in Photosystem II**

Simon Petrie, Rob Stranger and Ron J. Pace**

Section S1: Model Compound Descriptions

Table S1: Model Mn compound data of Dau et al., [17], showing oxidation states, ligand environment and $K\beta_{1,3} \langle E \rangle$ and E_0 values. Compounds 1-8 are mono or di-Metal (Mn_2 or Mn,Fe) Mn complexes (see [17], with representative structures given in Fig. S1 below). Compounds 9-11 are Mn oxides (indicated), with O_6 ligation. Compound 12 is a tetra Mn complex, with mainly O ligation (see [17]). Most Mn co-ordination is sixfold, but compound 5 is penta co-ordinate.

Compound ^[a]	Ox. States(s)	Ligands	$\langle E \rangle$ eV	E_0 ^[b] eV
1	(II) ₂	$Mn^{II}O_2N_4$	6491.49	6492.44
2	(III) ₂	$Mn^{III}O_6$	6490.86	6491.97
3	(III)	$Mn^{III}O_5N$	6490.85	6492.03
4	(III) ₂	$Mn^{III}O_4N_2$	6490.96	6492.14
5	(III)	$Mn^{III}O_3N_2$	6490.82	6491.82
6	(IV)	$Mn^{IV}O_4N_2$	6490.33	6491.08
7	(IV)	$Mn^{IV}O_3N_3$	6490.33	6491.14
8	(IV) ₂	$Mn^{IV}O_3N_3$	6490.40	6491.06
9	(III)	$Mn^{III}_2O_3$	6490.97	6491.88
10	(IV)	$Mn^{IV}O_2$	6490.25	6491.26
11	(II)	$Mn^{II}O$	6491.38	6492.34
12	(III-II) ₂	$(Mn^{II}Mn^{III})_2O_9Cl$	6491.24	6492.34

[a] As listed by Dau [17]. [b] Estimated from Fig. S4 in [17].

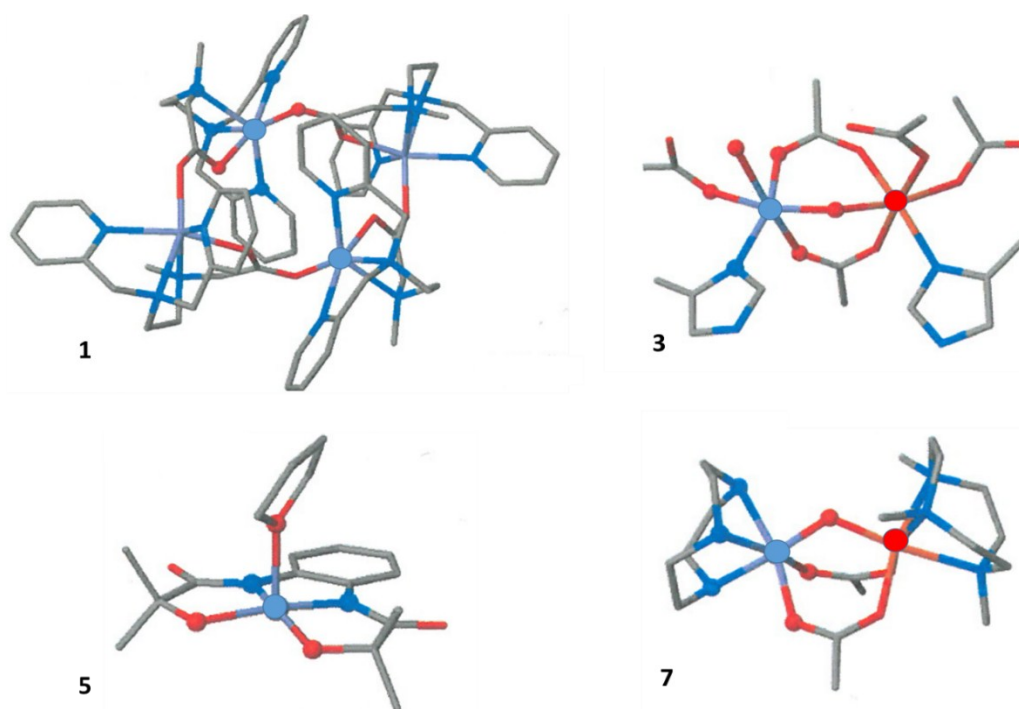


Figure S1: Structures of representative examples of O-N ligated Mn Compounds of Dau et al., used for $K\beta_{1,3}$ calibration in [17] (from Fig. S2 in Dau et al.). Compound 5 is 5-co-ordinate. Compounds 3,7 are mixed metal. Colour coding is; Mn (violet), Fe (bright red), O red, N (blue), C (grey). Protons omitted

Table S2: Model Mn compound data of Yachandra et al et al., showing oxidation states, ligand environment and $K\beta_{1,3} \langle E \rangle$ and E_0 values. Data from [12b] for oxo bridged dimeric complexes (compounds 1-5) and for oxo bridged trimeric and tetrameric species (compounds 6-9) [12d]. See Fig S2 below

Compound ^[a]	Ox. States(s)	Ligands	$\langle E \rangle$ eV	E_0 ^[b] eV
1	(III) ₂	MnO ₂ N ₄	6490.39	6491.32
2	(III,IV)	MnO ₂ N ₄	6490.18	6490.88
3	(IV) ₂	MnO ₂ N ₄	6489.96	6490.44
4	(III,IV)	MnO ₂ N ₄	6490.21	6491.12
5	(IV) ₂	MnO ₂ N ₄	6490.01	6490.70
6	(II,III) ₂	(Mn ^{III} O ₅ N)(Mn ^{II} O ₆)	6490.63	-
7	(III) ₃	MnO ₅ N	6490.51	-
8	(II,III) ₃	MnO ₄ N ₂	6490.54	-
9	(III) ₄	MnO ₄ N ₂	6490.45	-

[a] Compounds 1-3 mono μ -oxo bridged. Compounds 4-5 di μ -oxo bridged. [b] Estimated from Fig. 8 in [12b].

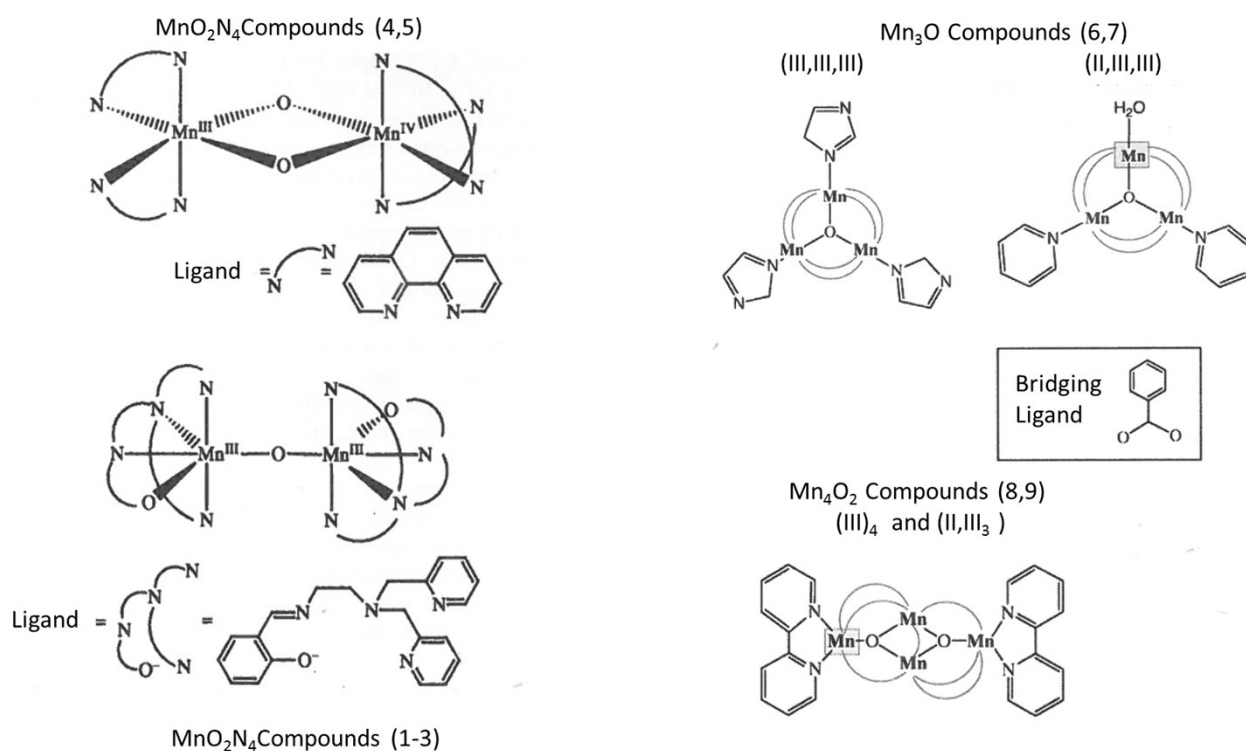


Figure **S2** Structure schematics for O-N ligated Mn Compounds of Yachandra et al., used for $K\beta_{1,3}$ calibration in Figs 4,5 present text. (From Fig. 2 in [12b] and Fig. 2 in [12d]). Numbering as in Table **S2** above. Protons omitted

Table S3: Model Mn compound data of Pushkar al et al. [12f], as for Tables **S1,2** above.

Compound ^[a]	Ox. States(s)	Ligands	<E> eV	E ₀ ^[b] eV
1	(III,IV)	MnO ₂ N ₄	6490.29	6491.19
2	(III,IV) ₂	MnO ₆	6490.42	-
3	(III-IV) ₂	MnO ₆	6490.43	-

[a] Compound 1 is equivalent to compound 4 in Table **S2**. Compounds 2,3 have tri μ -oxo bridging and tri phosphinate terminal ligation, see Fig **S3** below. [b] Estimated from Fig. 3 in [12f].

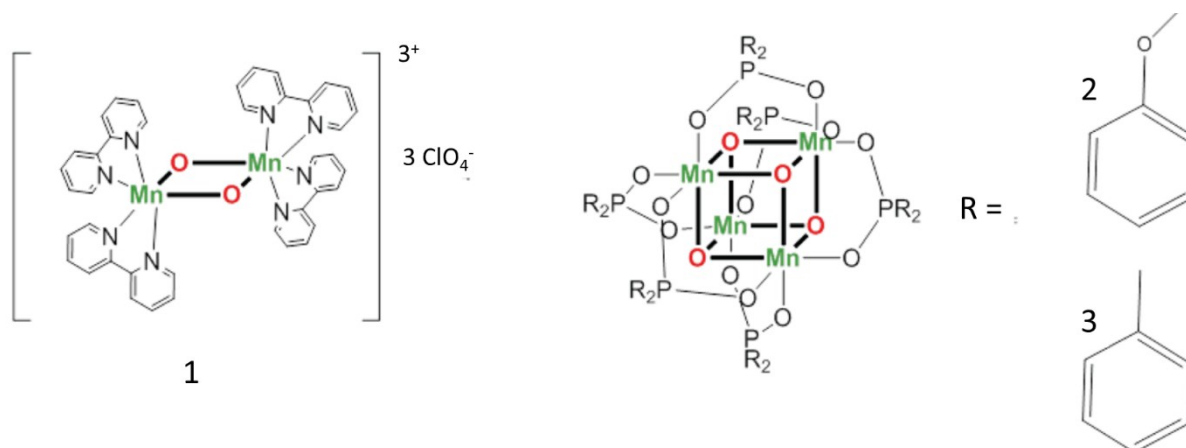


Figure **S3:** Structure schematics for O-N ligated Mn Compounds of Pushkar et al., used for $K\beta_{1,3}$ calibration in Figs 4,5 present text. (From Fig. 1 in [12f]). Numbering as in Table **S3** above. Protons omitted

Section S2: $K\beta'$ and Baseline Offset Effects

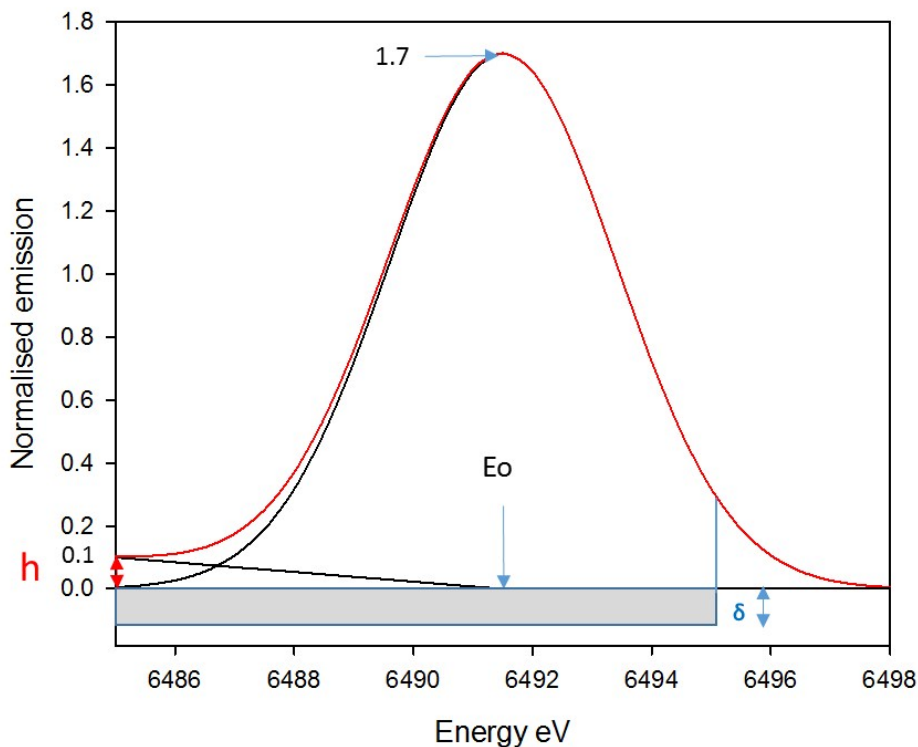


Fig. S4: Illustrates schematically the effects of the $K\beta'$ high energy wing intensity intrusion into the region of the $K\beta_{1,3}$ emission peak and baseline assignment position. The ‘pure’ $K\beta_{1,3}$ emission (black) is approximated as a simple Gaussian curve ($E_o = 6491.5$ eV, height $A_o = 1.7$ units, half height width = 4.5 eV). The $K\beta'$ edge is approximated as a ‘wedge’ of height h at 6485 eV, tapering to zero at E_o . The ‘true’ baseline for these goes through 0 on the emission axis. The blue rectangle, height δ , represents the additional emission, included in the $\langle E \rangle$ integral determination (from 6485 to 6495 eV), from variation in assigned baseline. Red curve is the total for $K\beta'$ and $K\beta_{1,3}$ intensities. The ‘true’ $\langle E \rangle$ value is E_o , ie 649.50 eV.

The quantitative effects of the $K\beta'$ and baseline effects for the above illustrative example, are indicated below:

let $E_o = (E_o - 6485) = 6.50$ eV here,

Then for the $K\beta'$ effect, the apparent shift ($\Delta\langle E_o \rangle$) in the estimated $\langle E \rangle$ value is given by :

$$\Delta\langle E_o \rangle \sim E_o - (h \cdot E_o^2 / 6 + \text{Area}_g \cdot E_o) / (\text{Area}_g + h \cdot E_o / 2) \dots\dots\dots 1)$$

where Area_g is the total area of the Gaussian curve up to the upper integration limit of 6495 eV. For the case above this is ~ 8.0 units (varies somewhat with E_o position)

For the baseline effect, the corresponding $\Delta\langle E_o \rangle$ value is given by :

$$\Delta\langle E_o \rangle \sim E_o - [(50 \cdot \delta + \text{Area}_g \cdot E_o) / (\text{Area}_g + 10 \cdot \delta)] \dots\dots\dots 2)$$

If $h \sim 0.1$ and $\delta/A_0 \sim 0.1$, (see main text), then both equations 1) and 2) separately predict $\Delta\langle E_0 \rangle$ values of ~ 0.2 - 0.3 eV, depending on the precise E_0 position, actual Gaussian width etc. In both cases, the perturbations produce an apparent $\langle E \rangle$ value which is **Lower** than the 'true' E_0 value, i.e. correspond to an apparently *Higher* Mn oxidation state.

Section S3: Turnover Difference Baseline Levelling

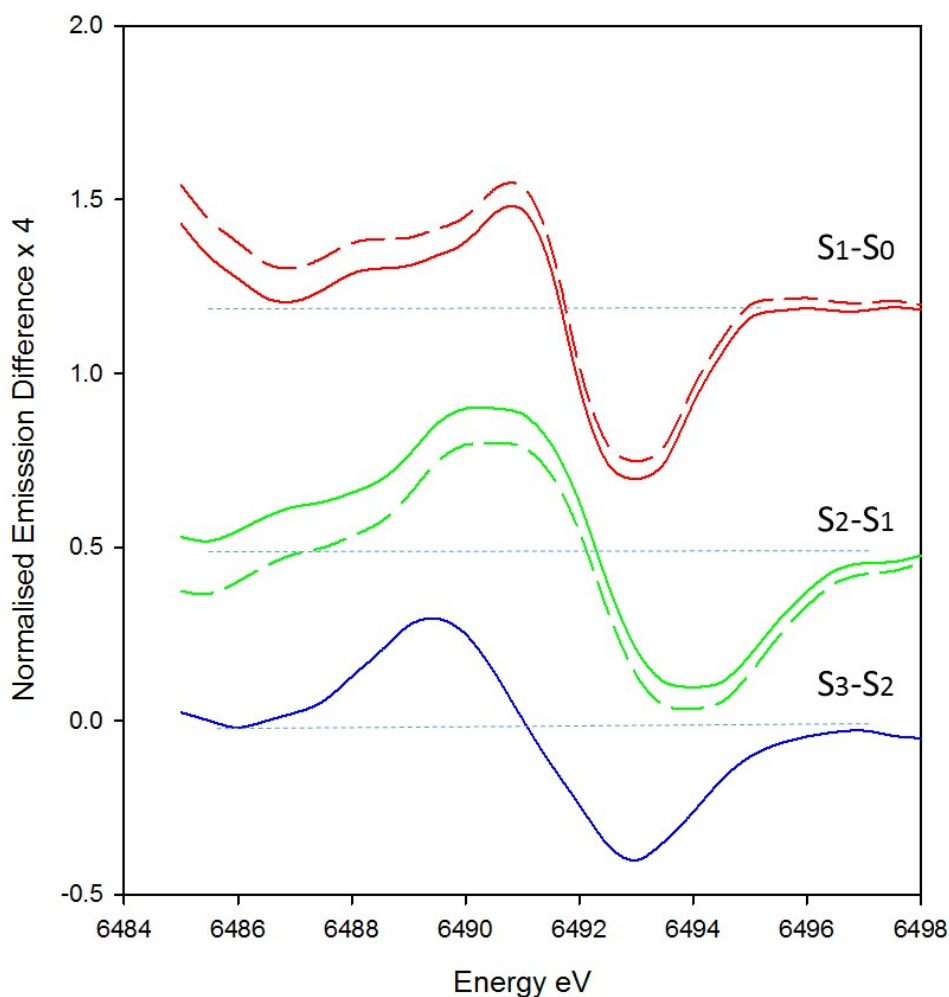


Fig. S5: Shows levelled curves (full) and raw unlevelled curves (dashed) for S state turnover difference spectra of Dau et al. [17] (see also main text). Levelling was by linear baseline adjustment, as indicated by dotted lines. This is reasonable for the S_2 - S_1 spectrum, but the S_1 - S_0 spectrum likely shows evidence of a non linear intrusion of $K\beta'$ intensity into the energy region below ~ 6488 eV, which is substantially greater in the S_1 spectrum than in the S_0 spectrum. This effect is essentially absent in the other two turnover difference spectra, suggesting that the extra $K\beta'$ intensity largely cancels between successive S states up to S_3 (i.e. is equally present in those states). All of these effects however, have very little influence on the estimation of the central inflection point energies (typically < 0.1 eV).

Section S4: PS II RIXS Data of Yachandra et al. [13].

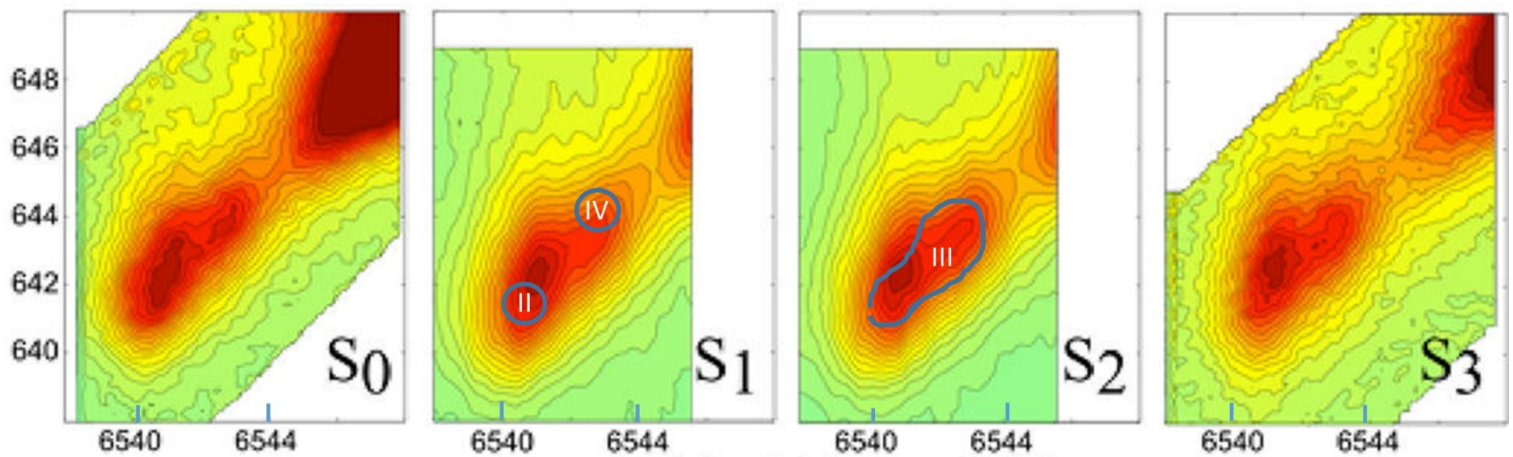


Fig S6: Reproduced Mn RIXS plots for the de-convoluted S states of PS II, with axis identifications as described in main text and refs [13]. Overlaid on the S₁ plot are the principal RIXS peak positions for Mn(II) (MnO) and Mn(IV) compounds from [13b], with mainly O ligation (see main text). The extended region overlaying the S₂ plot is for Mn₂O₃ (Mn(III)), from [13a].